Hybrid cyanine-silica nanoparticles: homogeneous photoemission behavior of entrapped fluorophores and consequent high brightness enhancement

UNIVERSITÀ DEGLI STUDI DI TORINO

Hybrid cyanine-silica nanoparticles: homogeneous photoemission behavior of entrapped fluorophores and consequent high brightness enhancement

Gabriele Alberto [a,c]*, *Ivana Miletto* [a,c], *Guido Viscardi* [b,c], *Giuseppe Caputo* [a,c],

Loredana Latterini [d], *Salvatore Coluccia* [a,c] *and Gianmario Martra* [a,c]

[a] Department of IPM Chemistry, University of Torino, Via Pietro Giuria 7, 10125 Torino (Italy)

[b] Department of General and Organic Chemistry, University of Torino, Corso Massimo D'Azeglio 48, 10125 Torino (Italy)

[c] NIS (Nanostructured Interfaces and Surfaces) Interdepartmental Centre of Excellence, at the Centre for Innovation, Via Quarello 11/A, 10135 Torino (Italy)

[d] Department of Chemistry and Nanostructured Innovative Materials Centre of Excellence (CEMIN), University of Perugia, Via Elce di Sotto 8, 06123 Perugia (Italy)

**Corresponding author:* Gabriele Alberto, gabriele.alberto@unito.it

Phone: +390116708384 Fax: +390116707855

ABSTRACT

Spherical hybrid cyanine-silica nanoparticles, quite homogeneous in size (ca. 50 nm) were prepared by the reverse microemulsion method. Solvatochromism tests indicated that all fluorophore molecules were actually entrapped within the inorganic matrix. The combination of steady-state and time resolved fluorescence measurements allowed to conclude that almost all cyanine molecules exhibited the same photophysical behavior and this suggested they should be dispersed in a monomeric form. Such behavior resulted in a significant brightness enhancement per nm^3 of nanoparticle with respect to molecules in solution. The occurrence of optical interparticle effect by progressively decreasing the distance among hybrid nanoparticles passing from suspension to a dry powder was also investigated.

KEYWORDS

dye-doped silica nanoparticles, steady-state and time resolved fluorescence spectroscopy, interparticle effects.

Introduction

Since the pioneering work of Stöber[1] the entrapment of organic fluorophores in silica nanoparticles (NPs) raised an increasing interest because of their higher photostability and emission intensity (brightness) with respect to the free molecules[2]. Such improved performances resulted from the prevention or reduction of the contact between fluorophores and molecular oxygen (responsible for photo-oxidation and, if the case, of collisional quenching), the increase of the photoemission quantum yield of entrapped molecules because of the loss of degree of freedom and the confinement of a high number of fluorescent molecules in a nanospace.

Because of these improved photophysical features, dye-doped silica NPs have been widely investigated as potential labels for biomolecules in diagnostic and imaging applications[3-7] and in forensic investigation[8,9]. Furthermore, their interesting optical scattering and interference effects render these systems very attractive for the design of photonic crystals and smart materials, such as Light Emitting Diode (LED) and Organic Light Emitting Diode (OLED), potentially employable for optoelectronic devices[10,11].

Different types of organic and metallorganic fluorophores have been considered, such as fluoresceine isothiocyanate (FITC), rhodamine 6G (R6G), pyrene, $RuII(bpy)_3$[6,7,12-16] and indocarbocyanine dyes. This last family of dyes is of particular interest because of the high molar extinction coefficient (of the order of 1.5×10^5 L $mol^{-1}cm^{-1}$) and the possibility to tune the absorption and emission maxima over a wide wavelength range by changing the length of the polymethine chain[17] and the number/type of substituents on the indoleninic rings. In particular, the possibility to up-shift the photoemission signal towards the longer wavelength region of the spectrum is relevant for biological applications, where the substrate can emit a "background fluorescence" spread over a wide range at lower wavelength[18].

In a previous paper[19], we reported that highly bright and photostable fluorescent nanoparticles can be obtained by adding a type of indocarbocyanine molecules conjugated with

aminopropyltriethoxysilane (APTS) among the reactants employed for the preparation of silica nanospheres by using the water in oil microemulsion method. In particular, the most relevant features of those NPs were the high photostability, the increase of ca. 13 times of the photoemission intensity of the cyanine molecules resulting from the hybridization with the inorganic matrix and the uptake of NPs by neuronal-like cells, that occurred even in the absence of any specific surface functionalization.

However, some questions still remained open, as the actual location of all cyanine molecules in the bulk of NPs and the degree of homogeneity of their photophysical behavior, that should reflect homogeneity in dispersion and environment. In this respect, here we report the results of solvatochromic tests and fluorescence lifetime measurements. In addition to these intraparticle aspects, we extended the investigation to possible interparticles optical effects, exploring the dependence of the intensity, shape and position of the cyanine loaded NPs photoemission on their dispersion. Such aspect attracted our attention because in practical applications the agglomeration/aggregation of NPs can occur unintentionally, as in biological media, or result from an engineered organization, as in photonic crystals[10,11]. At the best of our knowledge, no other studies of this kind have been reported in the literature dealing with fluorescent (silica) nanoparticles.

2. Experimental

2.1. Materials and syntheses

2.1.1. Parent cyanine. *IRIS3-NHS* (Fig.1a) was purchased by Cyanine Technologies S.r.l. (Torino, Italy). The cyanine employed contained also a phthalimido group introduced as amino-protecting group, to be cleaved and used for conjugation with carboxylic acid in other kinds of applications. All other reagents and solvents (cyclohexane, n-hexanol, ethanol, dimethylformamide, diethyl ether,

tetraethyl orthosilicate, APTS) were high purity grade Sigma-Aldrich products and used as received, as well as acetonitrile, 2-propanol and methanol used for the solvatochromism tests.

2.1.2. Synthesis of the IRIS3-APTS conjugate

The *IRIS3-APTS* (Fig. 1b) derivative was prepared by adding APTS (46.00 μmol; 10 μL) to a solution of the dye in DMF (11.5 μmol; 500 μL) and stirring for 24 hours at room temperature. The reaction was monitored by TLC and mass spectrometry (MS) to the complete conversion of *IRIS3-NHS* in *IRIS3-APTS*. The final product was finally separated from the unreacted APTS by dilution in diethyl ether and subsequent filtration, obtaining the product as a powder (purity assessed by MS: ESI-ION TRAP m/z=834 $[M-I]^+$)

Please insert figure1 here

2.1.3. Preparation of Pure (NPs) and IRIS3 loaded Silica Nanoparticles (IRIS3-NPs)

Silica nanoparticles were prepared by a W/O microemulsion method well established in the literature[16]. The microemulsion environment was prepared by mixing cyclohexane (75 mL), *n*-hexanol (18 mL), TX-100 (17.7 mL) and deionised water (5.4 mL). The mixture was gently stirred at room temperature for 30 minutes and then *IRIS3-APTS* (0.6 μmol; 0.2 mL) was added. After stirring for 10 minutes, tetraethyl orthosilicate (TEOS) (4.5 mmol; 1 mL) and NH_4OH (28-30%, 5.3 mmol; 0.7 mL) were added to start the hydrolysis and the condensation of the silane precursor. The reaction mixture was stirred for 16 hours at room temperature and then the reaction was stopped by the addition of acetone (40 mL). IRIS3-NPs were extracted by centrifugation and separated from the supernatant; subsequently nanoparticles were washed twice with absolute ethanol and several

times with deionised water to completely remove surfactant molecules. Samples were finally re-suspended in distilled water and stored at room temperature.

An aliquot of pure silica NPs were prepared by the same procedure, but without the addition of *IRIS3-APTS*.

2.2. Methods

2.2.1. Transmission Electron Microscopy (TEM)

TEM images were obtained with a 3010 Jeol instrument operating at 300kV. For the measurements, a droplet of the suspensions of IRIS3-NPs was spread on a copper grid coated with a perforated carbon film, and then the liquid was allowed to evaporate slowly, to limit the aggregation of NPs. The histogram of the size distribution of NPs was obtained by measuring ca. 300 particles, and the mean particle diameter (d_m) was calculated as $d_m=\Sigma d_i n_i/\Sigma n_i$, where n_i was the number of particles of diameter d_i. The results are indicated as ($d_m \pm$ STDV).

2.2.2. UV-Vis Absorption Spectroscopy

Electronic absorption spectra were collected with a Perkin Elmer Lambda 19 instrument equipped with an integrating sphere, coated with $BaSO_4$, for measurements on solid samples in the diffuse reflectance mode. The reflectance spectra were then converted in absorbance-like profiles by using the Kubelka-Munk function.

2.2.3. Photoluminescence Spectroscopy

Photoemission and excitation steady-state spectra were acquired with a Horiba Jobin Yvon Fluorolog3 TCSPC spectrofluorimeter equipped with a 450W Xenon lamp and a Hamamatsu R928 photomultiplier.

Fluorescence lifetimes, τ_F, were measured with a Spex Fluorolog-τ_2 system, by using the phase-modulation technique (excitation wavelength modulated in the 1± 300 MHz range; time resolution

ca. 20 ps). The frequency-domain intensity decays (phase angle and modulation vs. frequency) were analyzed with the Global Unlimited (rev.3) global analysis software.

3. Results and Discussion

3.1. Summary on shape, size and cyanine content of IRIS3-NPs

Figure 2 shows a representative TEM image of IRIS3-NPs, that appeared as well shaped spherical particles, with a quite narrow size distribution centered at ca. 50 nm (Fig. 2, inset). As reported in ref. (19), dynamic light scattering measurements indicated that in distilled water ca. 70% of such particles were individual objects, while the rest should form aggregates of 2-3 nanospheres. The same results were obtained for pure silica NPs. The mean NP volume derived from these data, combined with the converted amount of TEOS and the density of the IRIS3-NPs (corresponding to that of amorphous silica, ca. 2.2 g/cm^3)[20], allowed the estimation of the number of NPs in the suspension obtained at the end of the synthesis. Furthermore, on the basis of the amount of *IRIS3-APTS* conjugate that partecipated to the formation of the NPs (actually, all the initial dose), the average content in cyanine molecules per single NP was evaluated, as well as a formal "molarity" of IRIS3 molecules with respect to the suspension volume. This last parameter was of interest for the comparison with molecular solutions of IRIS3. The numeric values of all these features are listed in Table 1.

Please insert table 1 and figure 2 here

3.2. Photoemission behavior of IRIS3-NPs suspensions

3.2.1. Absorption and emission spectra of IRIS3-APTS

Normalized absorption (curve a) and emission (curve b) spectra of IRIS3 (identical to those of the derived IRIS3-APTS) in water are shown in Fig.3. The absorption profile exhibited a main contribution at 550 nm and an hypsochromic shoulder at 518 nm, while the photoemission spectrum is almost the mirror image, with the maximum located at 570 nm and the bathochromic shoulder at 600 nm. Because of the similarity with other polymethinic systems[21], these signals can be assigned to $\pi \rightarrow \pi^*$ transitions, with a partial charge transfer character, as the delocalization is extended to nitrogen atoms of the heterocyclic groups[22-25]. However, a general consensus on the origin of the different components in both absorption and emission spectra has not reached yet: most authors agree with the assignment of the main peak and ipsochromic/bathochromic shoulder in the absorption and emission spectra, respectively, to a vibronic structure[22,23,26,27a,28], as also reported in a recent review by Mustroph et al[29]. It is nevertheless true that some authors reported the possibility that they can be due to the *cis* and *trans* isomers of the cyanine molecule[31].

3.2.2. Solvatochromism tests

To assess the actual location of cyanine molecules in the NP_S, solvatochromism tests were carried out, by recording both the excitation (λ_{em}= 570 nm) and the emission (λ_{ex}= 500 nm) spectra of IRIS3 solutions and IRIS3-NPs suspension (concentration in the linear range of Fig. 5B, see after) prepared by using liquids with different polarity[32]. Excitation spectra were collected instead of the absorption ones, because the scattering by NPs prevented the possibility to carry out effective spectroscopic measurements in transmission. The obtained date are collected in Fig. 4, where it can be clearly observed that the spectra of IRIS3 in solutions exhibited the typical solvatochromic behavior expected for cyanine-type molecules[33] (section A), whereas those of IRIS3-NPs suspensions appeared completely insensitive to the polarity (section B) of the liquid medium. It was

then concluded that in the hybrid NPs all cyanine molecules were actually confined within the silica matrix and none of them was simply linked to the surface on the silica particles. This finding is in excellent agreement with the high photostability exhibited by IRIS3-NPs suspensions with respect to IRIS3 solutions[19]. However, other two aspects emerging from the comparison between the spectra of solution and suspensions deserve a comment. The first one deals with the difference in shape of the excitation spectra of IRIS3-NPs (section B, Exc) with respect to the molecular counterpart (section A, Exc): in the case of cyanine molecules entrapped in the silica matrix the shoulder gained in relative intensity with respect to the maximum, and a third weak component appeared at even lower wavelength. Conversely, the emission spectra of solutions and suspensions essentially exhibited the same shape (respectively sections A and B, Em side). By assuming the hypothesis that subbands in the abosprtion/exitation spetrum are due to a vibronic structure, it can be then proposed that the entrapment of cyanine molecules within the silica matrix induced a modification of the probability of transition to different vibrational levels of the excited electronic state.

The second aspect to be considered is the position of the components in the spectra of IRIS3-NPs, that appeared almost coincident with that obtained for IRIS-APTS dissolved in water. As the silica framework is conversely rather apolar[20], three explanations could be proposed: i) at the interface with the entrapped cyanine molecules, the silica framework exhibits polar defects, for instance $\equiv SiO^-$ species, also acting as counterions of the positively charged cyanines; ii) cyanine molecules and their counterions (I^-) are trapped to form ionic pairs[34], and iii) the electron clouds of the rigid surface of the "silica pockets" where the cyanine molecules are hosted represent a source of repulsion for the expanded electron clouds of cyanines in the excited state, with the consequent increase of its energy. Theoretical investigations in order to asses by modelling which among these hypotheses (if any) might actually account for the observed spectral position are in progress.

3.2.3. Fluorescent intensity and decay time of IRIS3-NPs

A wide series of IRIS3-NPs suspensions at different concentration was prepared, with a higher limit of $1.5x10^{14}$ NP/mL, beyond of which sedimentation started to occur. IRIS3 solution were kept in contact with air, because dissolved oxygen was expected to be a quite ineffective quenching agent towards fluorophores with lifetimes shorter than 5 ns[27b] as typically exhibited by cyanine dyes[35]. The photoluminescence spectra (λ_{ex} = 500 nm) were recorded, and their integrated intensity plotted as a function of both the suspension concentration (bottom X axis) and the amount of IRIS3 molecules present, expressed in molar concentration (top X axis), for the sake of comparison with cyanine actual solutions (Fig. 5). A monotonous behavior was obtained (section A), with a high linearity up to a concentration of $2.3x10^{13}$ NP/mL. The attention was then focused on that part (section B), where the shape of the emission spectra of the IRIS3-NP suspensions and of the IRIS3 solutions appeared almost identical (section C), indicating the absence of self-absorption of the emitted light by the cyanine molecules associated to the same NP. Conversely, as reported in our previous work[19], the intensity of the emission from the suspensions (full symbols, values on the left Y axis) appeared ca. 13 times higher than from the corresponding equimolar cianine solutions (open symbols, values on the right Y axis). Such an increase in intensity should be due to a significant increase of the quantum yield of molecules entrapped in the silica NPs. This increase of the quantum yield should be ascribed to the decreased occurrence of non-radiative relaxation processes in favour of the radiative ones, because of the loss of mobility.

Noticeably, such a remarkable increase in intensity, combined with the average number of cyanine molecules per NP, resulted in a "brightness enhancement per nm^3 of NP" that appeared ca. 10 times higher of that found by Larson et al. for rhodamine/APTS-NPs[36].

Beside fluorescence intensity, decay times were also measured, and the results are listed in Table 2. The frequency response curve of IRIS3 molecules in solution was satisfactorily fitted by a mono-exponential function, giving a decay time of 0.24 ns. The response curve of IRIS3-NPs

appeared slightly more complex, and the best fit was obtained by using a bi-exponential function. A small fraction (ca. 8%) of fluorophore molecules exhibited a decay time <0.05 ns, likely monitoring the formation of some poorly photoluminescent cyanine aggregates. Conversely, for the complementary 92% of fluorophore molecules the lifetime appeared increased of ca. 11 times with respect to IRIS3 in solution.

The close similarity between such increase in the decay time and the estimated increase in the fluorescence intensity per IRIS3 molecule (13 times) allowed to exclude the presence of significant amount of cyanine molecules entrapped in the silica matrix in a not-photo luminescent form (e.g. *cis* isomers and/or aggregates).

It can be then proposed that the overwhelming part of IRIS3 molecules is dispersed within each NP as single, highly photoluminescent molecules, all of them experiencing essentially the same type of environment. A basic condition favouring such dispersion should have been the very small *number of IRIS3/NP volume* ratio (ca 1.7×10^{-3} molecules/nm^3). However, more specific effects related to difference in molecular features (such as polarity) between IRIS3-APTS conjugate and TEOS used for building up the NPs could have ruled the relative rate of transport of the two types of molecular precursors through the interface of the reverse micelles, favouring the dispersion of IRIS3-APTS within the growing silica matrix. Specific investigations of this aspect, by using cyanine molecules functionalised with selected type and number of groups, are in progress.

3.2.4. Photophysical behavior of concentrated IRIS3-NPs suspensions, slurries, dry powders

As reported in Fig. 5, the dependence of the emission intensity on the amount of IRIS3-NPs in suspension started to deviate from the linearity for concentrations higher than 2.3×10^{13} NP/mL, with values of emission intensity progressively lower than expected. Such a behavior can be ascribed to the occurrence of effects of the inner filter type, likely combined with a progressively larger scattering of the excitation light as the amount of NPs increased. At presence, the evaluation of the

extent of each of these contribution was quite difficult. Noticeably, the suspensions were stable up to a concentration of $1.5x10^{14}$ NP/mL, whilst after such a limit the formation of sediment occurred in few minutes.

Besides the intensity, also the shape of the emission profiles started to deviate from that typical of IRIS3 molecules: by passing from the suspension with $2.3x10^{13}$ NP/mL (at the boundary between the linear and not-linear ranges of Fig. 5A) to that with $1.5x10^{14}$ NP/mL (the highest concentrated one), that produced spectra (a) and (b) in Fig. 6A, respectively, a slight shift of the maximum towards longer wavelengths and a gain in the relative intensity of the shoulder occurred. Such a trend further proceeded passing to the two slurries and the dry powder of IRIS3-NPs prepared to investigate the photophysical behavior of highly concentrated samples. Because of the complete lack of transparency, the emission spectra of these samples (Fig. 6A, c-d) were collected in the front face mode with respect to the excitation light. Such different optical condition prevented the possibility to compare the emission intensities of the suspensions with those of these three samples, whilst an internal comparison among these latter was still meaningful. It can be observed that by passing from the less concentrated slurry to the dry powder a decrease of the emission intensity occurred, accompanied by a further progressive red-shift of the maximum and loss in its relative intensity versus the shoulder, the two components finally exhibiting almost the same intensity (Fig. 6A, c-d). Whilst the decrease in intensity should be still partly due to an inner filter effect, the marked change in shape indicated the occurrence of self-absorption when IRIS3-NPs are in close contact, also contributing to the intensity decrease.

To evaluate the dependence of the self-absorption from the distance among cyanine loaded NPs in the dry state, the IRIS3-NPs powder was progressively diluted with pure SiO_2 NPs. The spherical shape of NPs and their narrow size distribution (see section 3.1) allowed to assume the dry powder as constituted by equivalent spheres, that could arrange in a close-packed structure. An example of the actual possibility that NPs can assume such packing is displayed in Fig.2 where a set of NPs arranged in a bidimensional hexagonal pattern can be observed. On such a basis, the first IRIS3-

NPs/pure SiO_2 NPs dilution ratio was of 1/12, that should statistically result in a shell of "white" NPs surrounding each dye-loaded NP. In the ideal case of a perfect hexagonal close-packing, the minimum distance between IRIS3-NPs should be of ca. 130 nm. The emission spectrum of this mixture appeared more intense that the signal produced by the IRIS3-NPs powder alone (Fig.6B, a,b), with significant gain in relative intensity of the main component versus the shoulder, resulting in a shape similar to that of the emission spectrum of the highest concentrated IRIS3-NPs suspension (Fig. 6A, b). A shape equivalent to that of the spectra of IRIS3-NPs suspensions in the linear range of Fig. 5 was obtained by attaining a dispersion ratio to 1:20 (minimum distance between IRIS3-NPs in a perfect hexagonal close-packing: ca. 365 nm), although with a marked decrease in intensity (Fig.6B,c).

Conclusions

The collection of results obtained indicated that the use of cyanine molecules and reverse micelles can lead to the formation of hybrid dye-silica nanoparticles where all fluorophore molecules, entrapped in the inorganic host, essentially exhibit the same photophysical behavior, witnessing for the absence of any aggregation, that could decrease the emission efficiency of the system.

Furthermore, the large enhancement of the emission intensity per molecule, significantly higher of those reported in the literature for other dyes and preparation methods, stimulates the prosecution of the research to attain the dye-loading limit that could be reached in order to maximize the brightness enhancement per nanoparticle, before the occurrence of detrimental dye-dye molecules intraparticle effects. Finally, the observed optical interparticle effects could be useful in becoming aware that, in practical applications the actual emission performances of fluorophores-hybrid nanoparticles can be well lower than expected, because of possible agglomeration. However, it

could be of interest to explore the possibility to exploit such interparticle effects to design devices based on the change of the emission intensity as a function of the distance among the fluorescent nanoparticles. Furthermore, the effect of packing of nanospheres with different diameters, as well as the possible energy transfer among NPs loaded with donors or with acceptors will be investigated as a prosecution of this work.

Acknowledgments

This work has been carried out in the frame of the Nanomat-ASP project (Docup 2000-2006, linea 2.4a). The Compagnia di San Paolo is acknowledged for financial support to NIS.

References and notes

(1) Stöber, W.; Fink, A.; Bohn, E. Controlled growth of monodisperse silica spheres in the micron size range. *J. Colloid Interface Sci.* **1968**, 26, 62-69.

(2) Yao, G.; Wang, L.; Wu, J.; Smith, J. Xu; Zhao, W.; Lee, E.; Tan, W. FloDots: luminescent nanoparticles. *Anal Bioanal Chem* **2006**, 385, 518-524.

(3) Sharma, P.; Brown, S.; Walter, G.; Santra, S.; Moudgil, B. Nanoparticles for bioimaging. *Adv. Coll. Interface Chem.* **2006**, 123, 471-485.

(4) Wang, L.; Zhao, W.; Tan, W. Bioconjugated silica nanoparticles: development and applications. *Nano. Res.* **2008**, 1, 99-115.

(5) Tansil, N.C.; Gao, Z. Nanoparticles in biomolecular detection. *Nanotoday*, **2006**, 1, 28-37.

(6) Yan, J.; Estévez, M.C.; Smith, J.E.; Wang, K.; He, X.; Wang, L.; Tan, W. Dye-doped

nanoparticles for bioanalysis. *Nanotoday* **2007**, 2, 44-50.

(7) Wang, L.; Wang, K.; Santra, S; Zhao, X.; Hilliard, L.; Smith, J.; Wu, Y.; Tan, W. Watching silica nanoparticles glow in the biological world. *Anal. Chem.* **2006**, 78, 646-654.

(8) Liu, L.; Gill, S.K.; Gao, Y.; Hope-Weeks, L.J.; Cheng, K.H. Exploration of the use of novel SiO_2 nanocomposites doped with fluorescent Eu 3+/sensitizer complex for latent fingerprint detection. *Forensic Sci. Int.* **2008**, 176, 163-172.

(9) Theaker, B.J.; Hudson, K.E.; Rowell, F.J. Doped hydrophobic silica nano- and micro-particles as novel agent for developing latent fingerprints. *Forensic Sci. Int.* **2008**, 174, 26-34.

(10) Yu Helmut, C.Y.; Argyros, A.; Barton, G.; van Eijkelenborg, M.A.; Barbe, C.; Finnie, K.; Kong, L.; Ladouceur, F.; McNiven, S. Quantum dot and silica nanoparticle doped polymer optical fibers. *Opt. Express* **2007**,15, 9989-9994.

(11) Hui, K.N.; Lai, P.T.; Choi, H.W. Spectral conversion with fluorescent microspheres for light emitting diodes. *Opt. Express*, **2008**, 16, 13-18.

(12) Rampazzo, E.; Bonacchi, S.; Montalti, M.; Prodi, L.; Zaccheroni, N. Self-Organizing Core-Shell Nanostructures: Spontaneous Accumulation of the Dye in the Core of Doped Silica Nanoparticles. *J. Am. Chem. Soc*, **2007**, 129, 14251-14256.

(13) Zhao, X.; Bagwe, R.P.; Tan, W. Development of Organic-Dye-Doped Silica Nanoparticles in a Reverse Microemulsion. *Adv. Mater.* **2004**, 16, 173-176.

(14) Santra, S.; Tapec, R.; Theodoropoulou, N.; Dobson, J.; Hebard, A.; Tan, W. Synthesis and Characterization of Silica-Coated Iron Oxide Nanoparticles in Microemulsion: The Effect of Nonionic Surfactants. *Langmuir* **2001**, 17, 2900-2906.

(15) Santra, S.; Liesenfield, B.; Bertolino, C.; Dutta, D.; Cao, Z.; Tan, W.; Moudgil, B.M.; Mericle, R.A. Fluorescence lifetime measurements to determine the core–shell nanostructure of FITC-doped silica nanoparticles: An optical approach to evaluate nanoparticle photostability. *J. Lumin*. **2006**, 117, 75-82.

(16) Santra, S.; Zhang, P.; Wang, K.; Tapec, R.; Tan, W. Conjugation of Biomolecules with Luminophore-Doped Silica Nanoparticles for Photostable Biomarkers. *Anal. Chem.* **2001**, 73, 4988-4993.

(17) Brooker, L.G. The Theory of the Photographic Process. New York: Ed. Macmillan, **1971**.

(18) Mishra, A.; Behera, R.K.; Behera, P.K.; Mishra, B.K.; Behera, G.B. Cyanines during the 1990s: A Review. *Chem. Rev.* **2000**, 100, 1971-2011.

(19) Miletto, I.; Gilardino, A.; Zamburlin, P.; Dalmazzo, S.;Lovisolo, D.; Caputo, G.; Martra, Viscardi, G.; Martra, G. Highly bright and photostable Cyanine dye-doped silica nanoparticles for optical imaging: photophysical characterization and cell tests. *Dyes Pigments* **2009**, in press, doi:10.1016/j.dyepig.2009.07.004

(20) Legrand, A.P. The Surface Properties of Silicas. New York. John Wiley, **1998**

(21) Koraiem, A.I.M.; Girgis, M.M.; Khalil, Z.H.; Abu El-Hamd, R.M. Electronic absorption spectral studies on new dimethine cyanine dyes. *Dyes Pigments* **1991**, 15, 89-105.

(22) Kachkovski, A.D.; Electronic properties of polymethine systems. 3: Polymethine and quasi-local electron transitions. *Dyes Pigments* **1994**, 24, 171-183.

(23) Kachkovski, A.D.; Dekhtyar, M.L. Electronic properties of polymethine systems. Part 4: Electronic structure of polymethine chain. *Dyes Pigments* **1996**, 30, 43-54.

(24) Kachkovsky, A.D.; Pilipchuk, N.V.; Kurdyukov, V.V.; Tolmachev, A.I. Electronic properties of polymethine systems. 10. Electron structure and absorption spectra of cyanine bases. *Dyes Pigments* **2006**, 70, 212-219.

(25) Tolmachev, A.I.; Romanov, N.N.; Fedotov, K.V.; Dyadyusha, G.G.; Kachkovski, A.D. A study of the vinylene shifts in polymethine dyes with sulphur-containing end-groups. *Dyes Pigments* **1988**, 9, 443-451.

(26) Bagwe, R.P.; Hilliard, L.R.; Tan, W. Surface modification of silica nanoparticles to reduce aggregation and nonspecific binding. *Langmuir* **2006**, 22, 4357-4362.

(27) Lackowitz, J.R. Principles of fluorescence spectroscopy. 3rd ed. Singapore: Springer; **2006** [a: Chapter 1, page 7-8. b: Chapter 19, page 629]

(28) Baraldi, I.; Caselli, M.; Momicchioli, F.; Ponterini, G.; Vanossi, D. Dimerization of green sensitizing cyanines in solution. A spectroscopic and theoretical study of the bonding nature. *Chem. Phys,* **2002***,* 275, 149-165.

(29) Mustroph, H.; Stollenwerk, M.; Bressau, V. Current Developments in Optical Data Storage with Organic Dyes. *Angew. Chem. Int. Ed*, **2006**, 45, 2016-2035.

(30) Mustroph, H.; Reiner, K.; Mistol, J.; Ernst, S.; Keil, D.; Hennig, L. Relationship between the Molecular Structure of Cyanine Dyes and the Vibrational Fine Structure of their Electronic Absorption Spectra. Chem. Phys. Chem, 2009, 10, 835-840.

(31) Sahyun, M.R.V.; Blair, J.T. Photophysics of a "simple" cyanide dye. *J. Photochem. Photobiol. A: Chem.* **1997**, 104, 179-187.

(32) The solubility of IRIS3-APTS varied in dependence on the solvent, as in the following scale: $CH_3CN > CH_3CH_2OHCH_3 > CH_3OH > H_2O$. In the last two cases the solubility was so low to prevent the possibility of an accurate determination of the concentration. As IRIS3-NPs suspensions the order of stability was: $H_2O > CH_3CH_2OH >> CH_3OH \cong CH_3CN$

(33) Bertolino, C.A.; Ferrari, A.M.; Barolo, C.; Viscardi, G.; Caputo, G.; Coluccia, S. Solvent effect on indocyanine dyes: A computational approach. *Chem. Phys.* **2006**, 330, 52-59.

(34) Tatikolov, A.S.; Ponterini, G.; Influence of ion pair formation on the photochemistry of asymmetric cationic indobenzimidazolo cyanines *J. Photochem. Photobiol. A :Chemistry*, **1998**, 117, 35-41.

(35) Terpetschnig, E ; Jameson, D.M. Fluorescence Lifetime (FLT). *ISS Technical Notes*. http://www.iss.com/resources/tech1/index.html

(36) Larson, D.R.; Ow, H.; Vishwasrao, H.D.; Heikal, A.A.; Wiesner, U.; Webb, W.W. Silica Nanoparticle Architecture Determines Radiative Properties of Encapsulated Fluorophores. *Chem. Mater.* **2008**, 20, 2677-2684.

Tables

Table 1. Quantitative features dealing with the synthesis of IRIS3-NPs
(the amount indicated are for a typical preparation)

Initial amount of TEOS (g)	TEOS converted in SiO_2 [a] (%)	average NP volume (cm^3)	NP density [b] (g/cm^3)	n. of NPs obtained	IRIS3-APTS molecules used[c]	IRIS3 molecules per NP
1	90.3	$6.54x10^{-7}$	2.2	$3.08x10^{15}$	$3.39x10^{17}$	110

[a] from ICP measurement of Si left in the supernatant at the end of the synthesis
[b] by gas picnometry
[c] then completely entrapped in NPs, see section 3.1

Table 2. Emission decay parameters of IRIS3 molecules in water solution ($1.0x10^{-6}$ M) and IRIS3-NPs water suspension ($1x10^{13}$ NPs/mL)

Sample	τ^0_F (ns)	χ^2
IRIS3	0.24 (100%)	0.99
IRIS3-NPs	2.63 (92%) ≤ 0.05	1.03

Figure Captions

Figure 1. Scheme of: a) IRIS3NHS, and b) IRIS3-APTS structures.

Figure 2. Representative TEM image of IRIS3-NPs (original magnification 40.000x); the white dashed-line evidences the hexagonal arrangement of some particles. Inset: histogram of the size distribution of NPs.

Figure 3. Optical spectra of IRIS3 in solution ($1.0 \cdot 10^{-6}$M), normalized at their maxima: a) absorption and b) emission (λ_{ex}: 500 nm).

Figure 4. Excitation (left) and emission (right) spectra, normalized at their maxima of IRIS3 molecules and IRIS3-NPs in different solvents. Section A, IRIS3 molecules dissolved in: a) water, b) methanol, c) 2-propanol [1.0×10^{-6} M] and d) acetonitrile [1.0×10^{-6} M] (see ref. 32). Section B, IRIS3-NPs suspended in the same series of solvents: all spectra resulted superimposed.

Figure 5. Section A: integrated photoemission intensities of IRIS3-NPs suspensions at increasing concentration. **Section B**: comparison of the photoemission intensities of IRIS3-NPs suspensions solution (full symbols) and IRIS3 solutions (open symbols) at different concentrations. **Section C:** comparison between representative normalized photoemission spectra of: a) IRIS3-NPs suspension and b) IRIS3 solution in the reported concentration range.

Figure 6. **Section A:** Emission spectra of: a) 2.3×10^{13} NP/mL and b) 1.5×10^{14} NP/mL IRIS3-NPs suspensions; c) 100 mg/mL and 200 mg/mL IRIS3-NPs slurries; e) dry IRIS3-NPs. **Section B:** Emission spectra of dry IRIS3-NPs: a) as such, the same as curve a in section A; b) diluted in pure SiO_2 NP, ratio= 1:12; c) diluted in pure SiO_2 NPs, ratio= 1:20

Figures

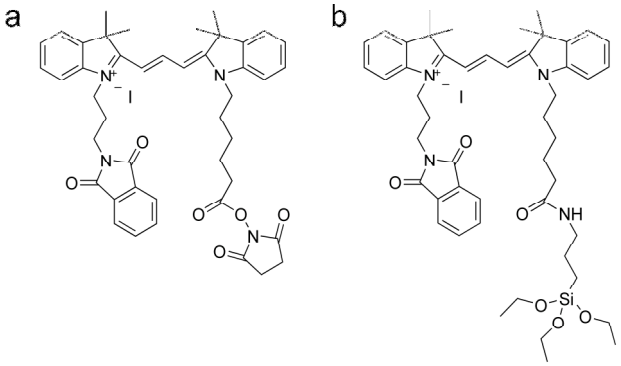

Figure 1

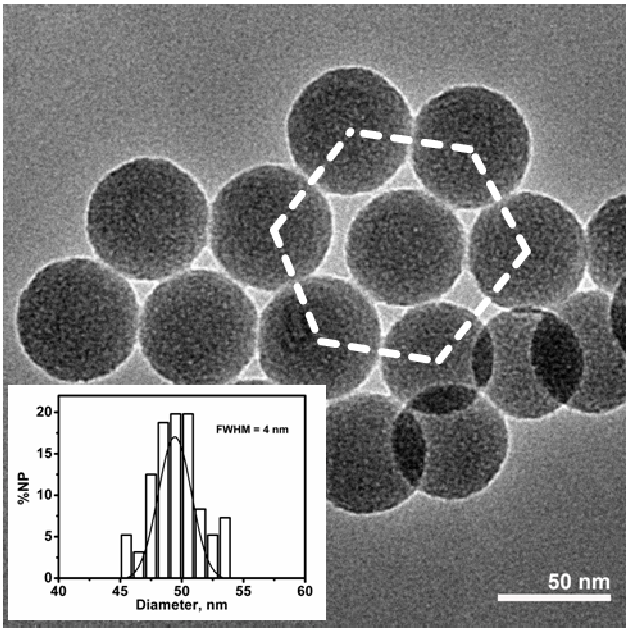

Figure 2

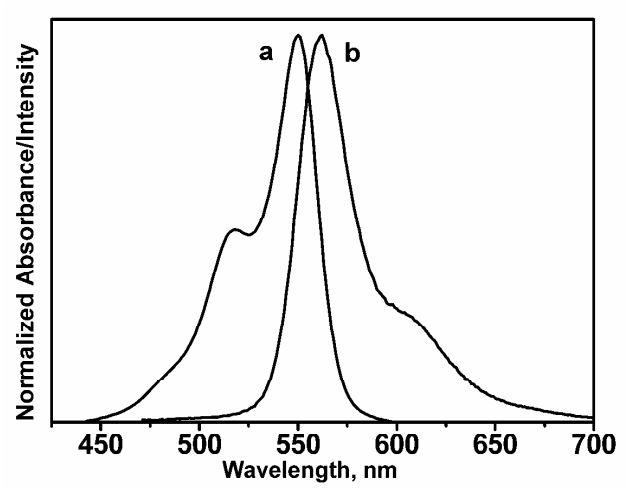

Figure 3

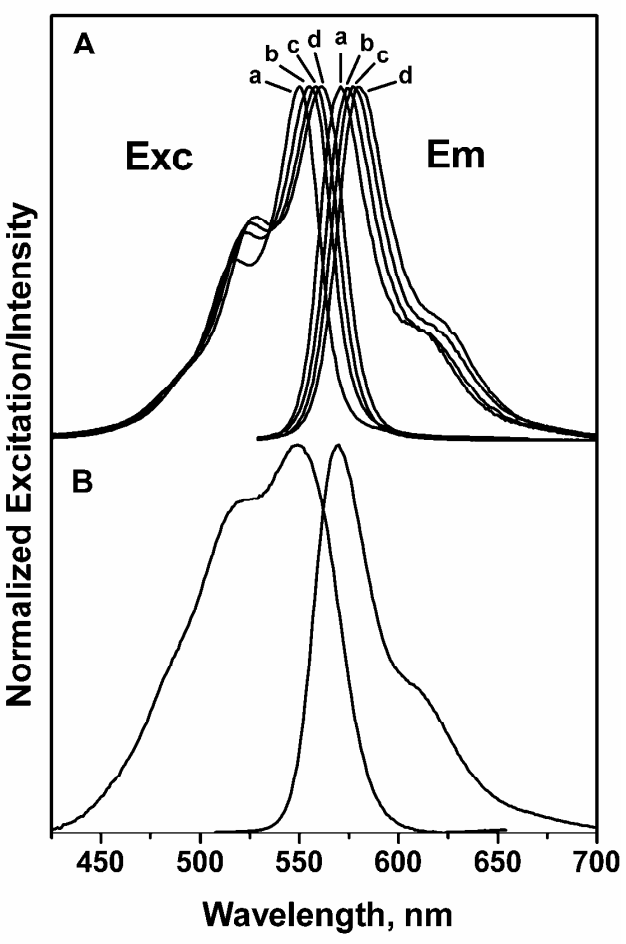

Figure 4

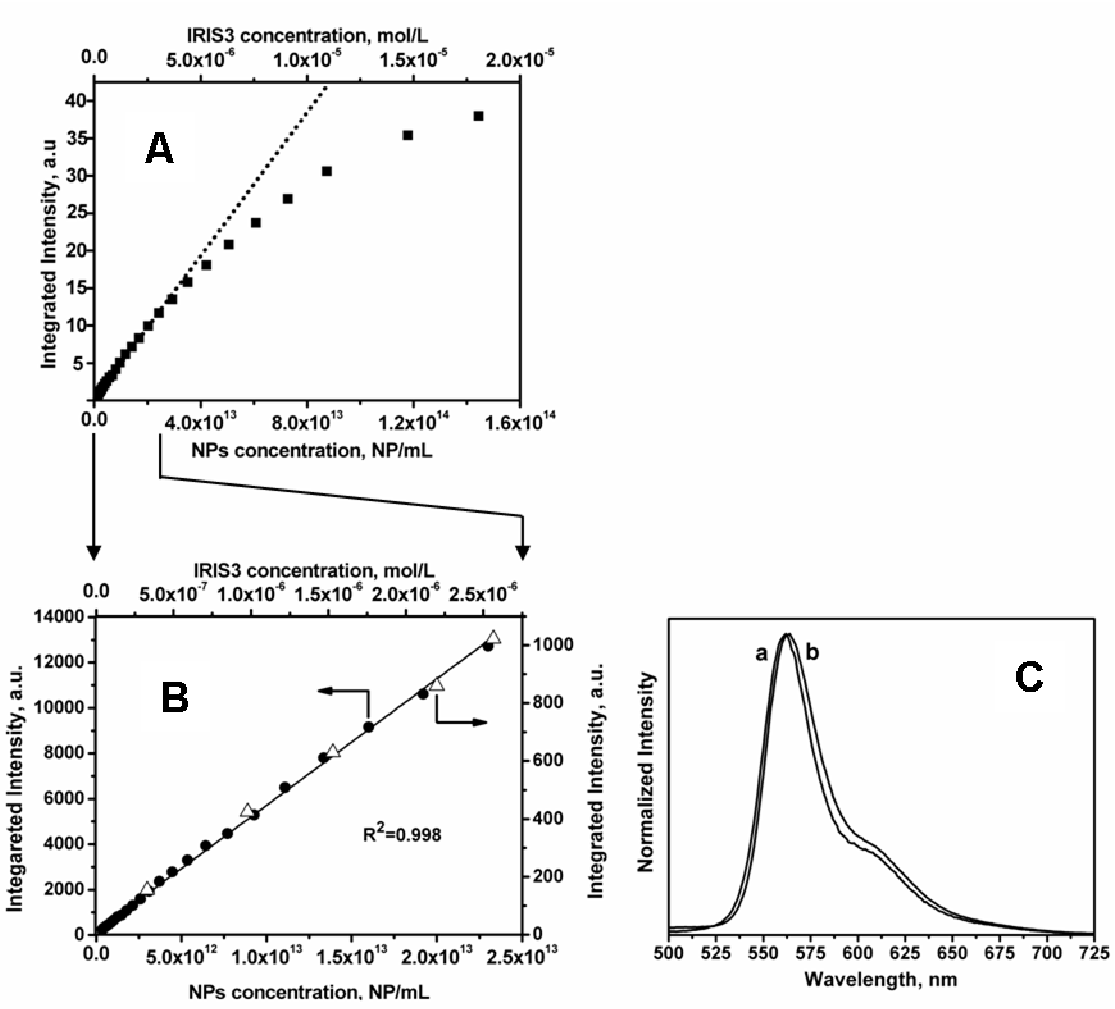
IRIS3 concentration, mol/L
0.0
5.0x10-6
1.0x10-5
1.5x10-5
2.0x10-5
A
Integrated Intensity, a.u
0.0
4.0x1013
8.0x1013
1.2x1014
1.6x1014
NPs concentration, NP/mL
IRIS3 concentration, mol/L
0.0
5.0x10-7
1.0x10-6
1.5x10-6
2.0x10-6
2.5x10-6
B
Integareted Intensity, a.u.
R2=0.998
Integrated Intensity, a.u.
0.0
5.0x1012
1.0x1013
1.5x1013
2.0x1013
2.5x1013
NPs concentration, NP/mL
a
b
C
Normalized Intensity
500 525 550 575 600 625 650 675 700 725
Wavelength, nm

Figure 5

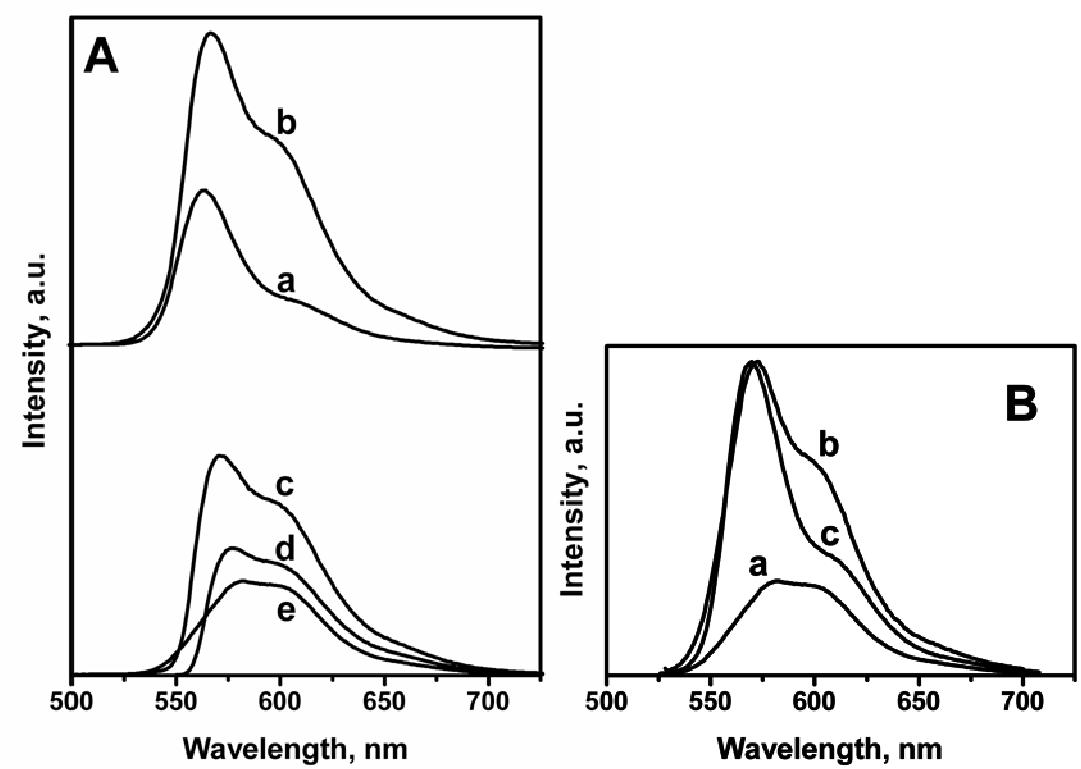
A
b
a
c
d
e
Intensity, a.u.
500
550
600
650
700
Wavelength, nm
B
b
c
a
Intensity, a.u.
500
550
600
650
700
Wavelength, nm

Figure 6